

Hydrogen Physisorption on the Organic Linker in Metal Organic Frameworks: Ab Initio Computational Study

Corneliu Buda and Barry D. Dunietz*

University of Michigan, Chemistry Department, 930 North University, Ann Arbor, Michigan 48109

Received: February 28, 2006; In Final Form: April 4, 2006

Research for materials offering efficient hydrogen storage and transport has recently received increased attention. Metal organic frameworks (MOFs) provide one promising group of materials where several recent advances were reported in this direction. In this computational study ab initio methods are employed to study the physisorption of hydrogen on conjugated systems. These systems are used as models for the organic linker within MOFs. Here, we focus on the adsorption sites related to the organic linker with special attention to the edge site, which was only recently reported to exist as the weakest adsorbing site in MOFs. We also investigate chemically modified models of the organic connector that result in enforcing this adsorption site. This may be crucial for improving the uptake properties of these materials to the goal defined by DOE for efficient hydrogen transport materials.

Introduction

The development of portable technology based on hydrogen fuel cells has promoted the need to design materials that can store large amounts of fuel, as hydrogen gas. The storage has to occur as close as possible to ambient temperature and pressure conditions as well as to allow small energetic barriers for "loading" and "unloading" the gas. A comparative study of modern hydrogen storage materials has been recently published.¹ Metal hydrides have been identified as one class of appropriate materials for the storage of hydrogen.^{2–5} However, there is still an array of problems associated with their use, which include cost, limited uptake, unfavorable unloading requiring heating, and high sensitivity to impurities. In addition, the large masses of these materials hinder the ability to improve their capacity. Alternative lighter materials are based on high-surface-area carbon materials.^{6–9} The carbon-based materials are used, however, with only partial success. These materials suffer from difficulty in reaching robust performance as structural uniformity is not obtained and the uptake mechanism is based on weak physisorption of the hydrogen (up to 2 kcal/mol adsorption energies).^{10,11}

One promising alternative class of materials for which several experimental successes have been recently reported is crystalline metal organic frameworks (MOFs).^{12–15} These materials are results of polymerization of metal ions with organic connectors. MOFs are a new class of materials, which offer high porosity and stability. MOFs are being widely explored as materials for a range of applications including catalysis¹⁶ and gas storage.^{17–20} For related reviews, see also refs 21–25.

Compared with alternative microporous materials, MOFs possess several strong advantages. MOFs can be flexibly designed through control of the architecture and functionalization of the building blocks. In addition, these materials are shown to be stable even when the pores have been emptied and heated.¹⁵ This high stability has been especially demonstrated for MOFs containing metal oxides. In addition, MOFs

offer the ability to control their structure and electronic distribution by varying the organic connector in the synthesis process. The important role of the organic connector for storage capacity was also demonstrated on a specific type of MOF, where $\text{Zn}_4\text{O}(\text{COO})_6$ clusters are used as the inorganic unit.^{17,19}

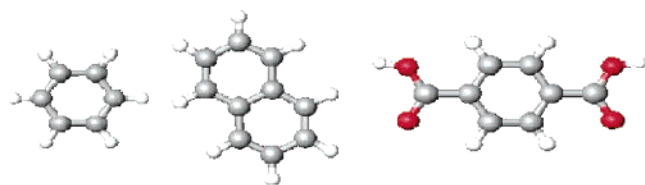
MOFs containing $\text{Zn}_4\text{O}(\text{COO})_6$ clusters as central units in the scaffoldings are among the materials whose significant hydrogen storage capability was demonstrated.^{17,19} It was also demonstrated that the uptake capability of these materials can be further enhanced by modifying the organic linker. Thus, the opportunity to engineer related MOF crystals emphasizes the potential to design even more efficient storing porous materials. Therefore, a clear understanding of the mechanism underlying hydrogen adsorption on the organic connectors is essential in optimizing the design of MOF materials for hydrogen storage.

The hydrogen adsorption sites in MOFs have been studied by inelastic neutron scattering (INS) techniques¹⁹ and Raman spectrometry.²⁶ These investigations point to the existence of well-defined binding sites, where each site can be associated either directly to the inorganic cluster or to the organic linker. This should be contrasted to other porous materials. INS studies on zeolites, for example, have found a broad distribution of binding sites.²⁷ The sites related directly to the inorganic cluster are found to have higher affinity to hydrogen than the alternative organic linker sites. It is expected that by improving the adsorption of the weaker organic sites the uptake properties of the MOFs may be enhanced. Therefore, in this study we concentrate on the weaker adsorption sites located at the organic linker. Computational models based on ab initio methods are used to provide insight on hydrogen adsorption on MOFs. Furthermore, we employ related models of a suggested chemical manipulation of the organic connector that can lead to improvement of the hydrogen uptake. Such structural changes may prove crucial in the effort to meet the hydrogen uptake goal set by the Department of Energy (DOE) of 6.5% uptake by weight.

Previous Computational Studies

A considerable number of computational studies regarding hydrogen molecules interacting with conjugated systems have

* Corresponding author. E-mail: bdunietz@umich.edu.



a) benzene b) naphthalene c) $\text{C}_6\text{H}_4(\text{COOH})_2$

Figure 1. Organic linker models (H, white; C, gray; O, red).

recently been published. The interaction energies and the corresponding geometries have been calculated at diverse levels of theory. These vary from DFT,^{28–30} to MP2,^{29–33} to CCSD and CCSD(T).³¹ The density functional theory (DFT) based studies involve a range of functionals, including special ones designed to address dispersion interactions.²⁸

Several of the available studies concentrate on carbon nanotubes that have been promoted as a leading type of material for hydrogen storage. Therefore, their focus was to model graphite-based systems as in the study of Heine et al.²⁹ This has resulted in a bias of the model with regard to the considered adsorption site, where graphite geometric bulk parameters were used in constrained optimizations of the adsorbed geometry. This choice is less appropriate when considering MOFs. Furthermore, the main focus of these studies was naturally only the top site. In this orientation the hydrogen molecule is pointed toward the center of the benzene plane being the available site for carbon nanotubes. The top site has been also the focus of other studies specifically aimed at modeling the organic linker adsorption sites within MOFs.^{32,33} The stability of the top site versus alternative orientations underlies the focus of these studies. Hubner et al.,³¹ for example, found the edge site of a fluorinated benzene ring to be less stable by about 3.0 kJ/mol than the most stable top site at the MP2/TZVPP level of theory.

As outlined above, prior computational work has focused on the interaction of hydrogen molecule with the top site of the conjugated systems. However, based on recent experimental evidence of hydrogen adsorption in MOFs,¹⁹ we have also considered the possibility of adsorption at the edge site. In this orientation the hydrogen molecule is facing the “side” of the ring. These edge sites become available in porous materials like MOFs, while they are absent in closed volume materials as with carbon nanotubes.²⁰

In this study we employ models to explain experimental observations on existing materials. In the following section, we describe the implementation of the calculations addressed to simulate the interaction of the MOFs with the hydrogen molecule at the sites related to the organic linker. We first describe the models used to represent the adsorption site and then the methodologies used to evaluate the interaction of the hydrogen molecule at the considered sites. Furthermore, we also suggest a chemical manipulation of the organic linker which is predicted to result in improvement of the hydrogen uptake properties of the related MOFs.

Computational Methods

Several models, illustrated in Figure 1, were employed to describe the organic linker within MOFs. Our simplest model of the organic linkers consists of a single benzene ring (Figure 1a). Adsorption geometries were optimized at the MP2 level with varying basis sets and at the B3LYP³⁴ level with the aug-cc-pVDZ³⁵ basis set. Geometry optimized structures at the relatively small TZV³⁶ basis set level were used as initial guesses

for optimizations at the larger basis set levels. We first consider the MP2 optimized structures calculated with the smaller basis sets of the considered hierarchy. These basis sets involve the cc-pVDZ basis set augmented with diffuse functions (aug-cc-pVDZ) and the cc-pVTZ.³⁵ The larger basis sets include the aug-cc-pVTZ and cc-pVQZ basis sets.³⁵ Calculations implementing MP2 theory with these larger basis sets are achieved by employing the resolution of the identity (RI).^{37,38} In addition, RI-MP2 was applied with the same smaller basis sets to allow benchmarking the RI-MP2 scheme to canonical MP2 theory. RI-MP2 was also used to extend the applicability of MP2 theory to the larger considered molecular models as described next.

The adsorption sites were also studied using larger models of the organic linker. A two-ring model (the naphthalene molecule shown in Figure 1b) was used to study the effect of varying the size of the conjugated system on the adsorption energy. In addition, extended models of the organic linker within MOFs have also been employed. These models include the dicarboxylated ring (Figure 1c). The adsorption energies and geometries of these extended molecules were calculated by employing the RI-MP2 scheme with the cc-pVTZ and aug-cc-pVDZ basis sets.

The hydrogen adsorption energy is defined as the difference of the adsorbed optimized geometry from the sum of the isolated species. Most of the calculated adsorption energies were corrected for the basis set superposition error (BSSE) using the counterpoise correction scheme.³⁹ It is also important to note that RI-MP2 calculations are limited by the availability of preexisting auxiliary basis sets.⁴⁰ All MP2 calculations were performed using GAMESS,⁴¹ except for the aug-cc-pVDZ basis set where the Q-Chem 2.1 package⁴² has been used. The calculations involving RI-MP2 approximation were carried out using Q-Chem 3.0.⁴³ We have also implemented B3LYP calculations with the Jaguar 5.5 package.⁴⁴

Results and Discussion

One-Ring Models. We first consider the interaction of hydrogen molecules with a single conjugated ring as a simple model for the MOF uptake of hydrogen molecules. The benzene ring is the organic linker within the MOF-5 material.⁴⁵ Figure 2 provides an illustration of both the top site (Figure 2a) and edge site (Figure 2b) of a benzene ring. Also illustrated are adsorption sites with a chemically modified ring (Figure 2c,d, see below). The illustrated geometries in Figure 1 are the result of full optimization at the MP2 level using the aug-cc-pVDZ basis set. Full geometry optimizations were also employed with the cc-pVTZ basis set at the MP2 level. In addition, RI-MP2 optimizations were performed at both basis sets. Therefore, we are able to benchmark the performance of RI-MP2 against canonical MP2 for the small one-ring models. The calculated interaction energies for the one-ring models are provided in Table 1, where the different considered levels of modeling are listed. Also listed in the table are the BSSE-corrected bond energies and their bond lengths.

Three different orientations for each of the top and edge sites have been considered. The most stable geometry for each site is illustrated in Figure 2. The most stable top sites have the hydrogen molecule pointing toward the middle of the benzene ring as in Figure 2a,c, where the hydrogen molecule is more tilted with the modified ring (Figure 2c). The other two considered top geometries involve parallel orientation of the hydrogen molecule to the ring forming a plane either with two opposite C atoms or with the center of two opposite carbon–carbon bonds. We have found small rotational barriers leading

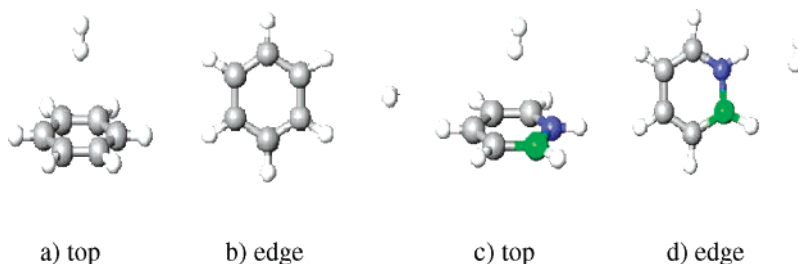


Figure 2. Optimized geometries for one-ring models at MP2/aug-cc-pVDZ level of theory. The plain ring sites are provided in parts a (top) and b (edge). The corresponding sites with the modified ring are illustrated in parts c and d.

TABLE 1: Adsorption Energies and Bond Distances for One Ring Model Species

level of theory/basis set	benzene				benzene—B,N			
	edge site		top site		edge site		top site	
	energy/ BSSE (kJ/mol)	H—H (Å)	energy/ BSSE (kJ/mol)	C—H (Å)	energy/ BSSE (kJ/mol)	H—H (Å)	energy/ BSSE (kJ/mol)	N—H (Å)
MP2/cc-pVTZ	−1.46	2.9	−4.66	3.0	−2.62	2.4	−4.54	3.1
MP2/aug-cc-pVDZ	−3.39	2.7	−8.83	2.9	−4.79	2.3	−7.46	2.9
RI-MP2/cc-pVTZ	−1.46/−1.09	2.9	−5.53/−3.56	3.0	−2.77/−2.18	2.4	−5.06/−3.51	3.0
RI-MP2/cc-pVQZ (sp)	−1.67	2.9	−5.14	3.0	−3.04	2.4	−4.90	3.0
RI-MP2/aug-cc-pVDZ	−3.39/−1.17	2.7	−8.85/−3.51	2.9	−4.79/−2.51	2.3	−7.47/−3.60	3.0
RI-MP2/aug-cc-pVTZ	−2.88/−1.55	2.7	−9.89/−4.14	2.9	−4.47/−2.93	2.2	−7.45/−4.35	2.9
B3LYP/aug-cc-pVDZ	−0.57/0.75	2.8	−0.16	3.3	−1.51/−0.71	2.4	−0.61	3.3

to the most stable top site from these alternative orientations in agreement with previous studies focusing on the top site.

The hydrogen orientation at the top site of the benzene modified model C_4BNH_6 (Figure 2c) is very similar to the one found for benzene ring (Figure 2a). However, we find a larger difference for the edge sites for the different models. In the most stable edge site orientation of the benzene ring model, the hydrogen molecule lies perpendicular to molecular plane facing a C—C bond (the hydrogen atoms are situated across the opposite side of the ring as illustrated in Figure 2b). In the corresponding edge site of the modified ring model, the hydrogen molecule is shifted into the ring plane toward the hydrogen atom bonded to the nitrogen atom (Figure 2d). In the other considered edge orientations the hydrogen molecule lies in the ring plane to be either parallel or perpendicular to a C—C bond.

In the discussion below involving larger models and basis sets, we concentrate on these most stable identified orientations. It is interesting to note that for the edge site the TZV basis set fails to accurately order the interaction energy of the alternative edge orientations. The TZV actually finds the “head-on” in-plane edge orientation to be lower than the identified lowest orientation described above. This reversal of the order of orientations is not noted for the top site but is, however, an illustration of the small rotation barriers predicted for both of these sites.

The identified adsorption geometries were further studied with the larger basis sets by employing the RI-MP2 approach. RI-MP2 was shown to well reproduce full MP2 results. In a recent study, for example, RI-MP2 faithfully reproduced binding energies of stronger electrostatic interacting species involving conjugated systems.⁴⁶ This study, however, involves weaker dispersion interactions. A first important observation provided by the table, therefore, confirms the ability of the RI-MP2 approach to accurately reproduce canonical MP2 results for such systems as well. In this study, all the reported benchmark results of RI-MP2 compare almost exactly against the canonical MP2 calculations for the aug-cc-pVDZ basis set. Bigger but still acceptable errors are noted for the cc-pVTZ basis set, where RI-MP2 predicts up to 0.88 kJ/mol stronger adsorption energies

than MP2 for the top site. Furthermore, the BSSE was corrected to achieve faster convergence of the basis set expansion.

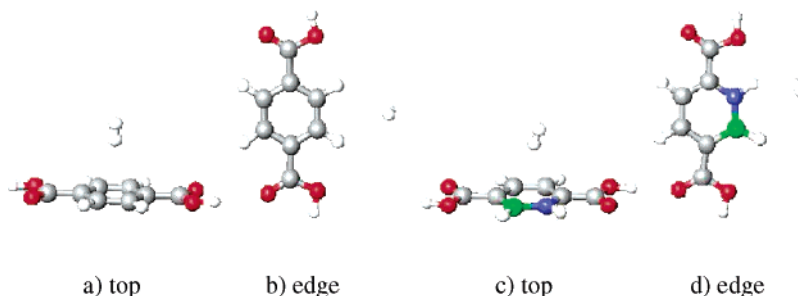
The BSSE-corrected results for the considered basis set expansions are within 0.85 kJ/mol of each other. This range is further reduced if only the augmented basis sets are considered to 0.40 kJ/mol for the edge sites or 0.75 kJ/mol for the top sites. In addition, the BSSE-corrected energy for the top site of the benzene ring (at the aug-cc-pVTZ basis set level) of 4.14 kJ/mol compares well with the basis set limit extrapolated result of 4.77 kJ/mol calculated by Sagara et al.³² Therefore, the full counterpoise scheme seems to overcorrect the BSSE by about 0.60 kJ/mol.

The MP2 results of the plain benzene ring are also in good agreement with available experimental results. In a recent experimental study of the different adsorption sites,⁴⁵ the edge site of the organic linker was interpreted as the site with the weakest interaction. Our RI-MP2/aug-cc-pVTZ results find the edge site to be less stable by 2.60 kJ/mol than the top site. In their study, Hubner et al.³¹ find the adsorption energy of the edge site to lie 3.0 kJ/mol above that of the top site, which was calculated to be 3.58 kJ/mol. Their comparison, however, was limited to C_6H_5F species using the smaller TZVPP basis set.

Next we consider the results obtained with the modified benzene ring. In this suggested chemical manipulation⁴⁷ the organic linker involves a cyclic conjugated system of six atoms, where a pair of carbon atoms is replaced by an isoelectronic pair of boron—nitrogen atoms. BN materials have been also used for hydrogen storage material with some success elsewhere.⁴⁸ The corresponding orientations of the adsorbed hydrogen on this system are illustrated in Figure 2b, and the bond distances and adsorption energies are also listed in Table 1. The most important observed trend is the enhanced interaction of the edge site when compared to the plain benzene ring performance. Namely, the modified ring is shown to increase the interaction energy of the weaker site. The adsorption energy calculated at the RI-MP2/aug-cc-pVDZ level of theory for the edge site increases from 1.17 kJ/mol with the plain benzene ring to about 2.51 kJ/mol with the chemically modified ring. On the other

TABLE 2: Adsorption Energies and Bond Distances for Extended Model Species

level of theory/basis set	benzene-2COOH				benzene-B,N-2COOH			
	edge site		top site		edge site		top site	
	energy/ BSSE (kJ/mol)	H-H (Å)	energy/ BSSE (kJ/mol)	C-H (Å)	energy/ BSSE (kJ/mol)	H-H (Å)	energy/ BSSE (kJ/mol)	N-H (Å)
RI-MP2/cc-pVTZ	-1.74/-1.26	2.8	-5.62/-3.18	3.0	-6.87/-5.86	2.3	-14.78/-13.01	3.0
RI-MP2/aug-cc-pVDZ	-4.07/-1.42	2.7	-9.13/-3.26	2.9	-9.13/-5.94	2.2	-17.24/-12.43	2.9

**Figure 3.** Optimized geometries for the carboxylated models using RI-MP2/aug-cc-pVDZ. The modified ring model sites are illustrated in parts c and d.

hand, the stronger top site adsorption energy, calculated at similar level of theory, remains almost unaltered at 3.60 kJ/mol.

We also include in the same table hybrid DFT results. DFT unfortunately suffers from well-documented limitations for describing weak nonbonded interactions.⁴⁹ Nevertheless, this method has also been used previously in the context of hydrogen physisorption calculations.^{28–30} Therefore, benchmarking well the ability of DFT to (accidentally?) reproduce trends related to the physisorption is in place. The benchmarking uses comparison of the calculated adsorption at the DFT level with more reliable methods for these systems such as MP2. This may prove especially helpful when larger models are considered.

Here, the first noted failure of DFT is the reversal of the adsorption site strength. Hybrid DFT is shown to prefer the edge site with a very weak interaction predicted. Furthermore, with the BSSE corrected no adsorption of either sites of the plain benzene ring is predicted anymore. On the other hand, DFT is able to reproduce the MP2 enhancement of the edge site adsorption for the modified ring system, where the calculated prediction for the enhancement of the top site adsorption is much smaller, in agreement with the MP2 prediction. In addition, the optimized geometries obtained by both methods are in good agreement.

The bond distances and energies calculated by the different models are listed in Table 1. The bond distances agree pretty well among the different considered levels, even comparing MP2 results with DFT calculations. For example, the hydrogen molecule at the edge site is predicted by both DFT and MP2 theories to be perpendicular to the plane. A difference in the orientation of the hydrogen molecule at the top site of the modified ring is noted, where a larger tilt angle is predicted with the DFT optimization. Previously, Hamel and Cote³⁰ by comparing DFT, MP2, and CCSD calculations were able to demonstrate the ability of DFT to reproduce qualitatively well the estimates for the top site rotational energy barriers predicted by the more appropriate methodologies.

As a final observation on the one-ring models, we provide estimates for the rotational energy barriers of the hydrogen at the edge site. Optimizations of the alternative edge site orientations with the plain ring have converged to stationary points different from the identified most stable geometries discussed above. These are the saddle points, which connect

the two equivalent edge orientations with the hydrogen molecule lying in the plane pointing head-on to a carbon-carbon bond. These geometries lie only slightly higher in energy than the most stable identified orientation, within a 0.25–0.46 kJ/mol range (depending on the basis set) of the BSSE-corrected adsorption energies. This result well complements the study of H₂ rotational energy barriers,²⁸ which was limited, however, to the top site of the benzene ring.

Extended Models. In real MOFs the inorganic Zn clusters are bonded through carboxylate groups by the organic conjugated linker. The simplest model to represent this is defined by the dicarboxylated benzene system, C₆H₄(COOH)₂. This model molecule is drawn in Figure 1c.

Previous studies have demonstrated the ability of these models to reproduce qualitatively results obtained by models with explicit inorganic atoms. This was demonstrated recently by Hubner et al.,³¹ who have employed RI-MP2 calculations on extended models. Their focus again was the top site. In their calculations several models including C₆H₄(COOH)₂ and C₆H₄(COOLi)₂ have been compared to the plain benzene ring model. Sagara et al.³³ have also demonstrated the ability of these models to reproduce qualitatively results obtained by models with explicit inorganic atoms.

In Table 2 the calculated energies and bond lengths of the carboxylated model are provided. The optimized geometry of the top and the edge sites of C₆H₄(COOH)₂ are illustrated in Figure 3a,b. The corresponding sites for the modified ring model C₄BNH₄(COOH)₂ are drawn to the right in Figure 3c,d. First, we note that the polarization effects due to the extended modeling influence only slightly the adsorption energies of the top site with the plain ring model. This is in good agreement with previous studies focusing on the top site.³¹ Furthermore, our results provide a similar observation for the edge site.

However, a strong influence of the carboxylate groups is demonstrated when the modified ring model is considered. In Table 2 we have also listed the adsorption energies of the hydrogen molecule at the edge and top sites of the dicarboxylated molecule with the B-N modification of the conjugation skeletal (illustrated in Figure 3c,d). The interaction enhancement shown with this modification is demonstrated for both sites and to a much larger extent than observed for the one-ring models. The adsorption energy for the top site is increased from 3.60 to 13.01 kJ/mol and that for the edge site is increased from 2.51

TABLE 3: Adsorption Energies and Bond Distances for Two-Ring Model: Naphthalene

level of theory/basis set	edge site (1)		edge site (2)		top site	
	energy/ BSSE (kJ/mol)	H–H (Å)	energy/ BSSE (kJ/mol)	H–H (Å)	energy/ BSSE (kJ/mol)	C–H (Å)
RI-MP2/aug-cc-pVDZ	−3.74/−1.26	2.6	−3.58/−0.79	2.7	−10.01/−3.89	2.9

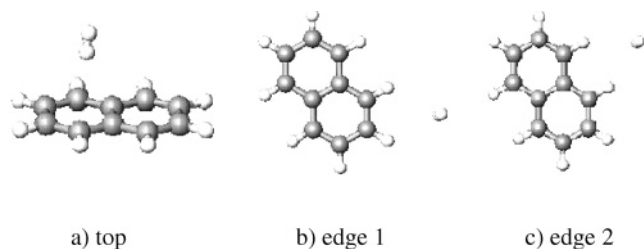


Figure 4. Optimized geometries for two-ring models using RI-MP2/aug-cc-pVDZ.

to 5.94 kJ/mol, after BSSE corrections. Also, the edge site bond distance is reduced by 0.5 Å, while the top site geometry remains almost unaltered. These are substantial enhancements of the adsorption energies and may result in better loading of the weakest adsorption sites in current existing MOFs.

Two-Ring Models. To study the effect of extended-conjugation linkers, we have calculated the adsorption energies of the edge and top sites with naphthalene at the RI-MP2/aug-cc-pVDZ level. Figure 4 illustrates the resulting optimized structures. The corresponding top site is shown in Figure 4a, and the edge site similar to the one found for the one-ring model is drawn in Figure 4b. We have also considered an alternative edge site formed by the larger two-ring system. This “new” edge site is defined by two hydrogen atoms that each belong to a different ring and is illustrated in Figure 4c. In Table 3 we list the calculated adsorption energies and bond lengths of these adsorption sites.

Our calculations show that extending the conjugation system leads to only small enhancements of the adsorption energies for both sites and marginal modification of the dispersion bond length. For example, the adsorption energy calculated for top site at the two-ring model increased by 0.38 kJ/mol relative to the benzene ring model. This reproduces previous results for the top sites, where modifying the conjugation systems from one ring to two rings has resulted in an increase of the calculated MP2 adsorption energy for about 0.35–0.40 kJ/mol.^{28,29,31}

Furthermore, the small interaction enhancement due to the extended conjugation system is predicted to be even smaller for the edge site. Only a marginal improvement of 0.10 kJ/mol is calculated for the edge site. Therefore, increasing the conjugation system is not predicted to substantially increase the adsorption energies of the organic sites. We also note that the alternative considered edge site involves a much weaker adsorption site with a 0.50 kJ/mol reduction of the adsorption energy when comparing both edge sites. This site, however, may become more important when other adsorption sites located at the inorganic cluster become loaded. Future studies should concentrate on the possible relation of these sites to the neighboring inorganic sites. This investigation may be beneficial for enabling more efficient uptake by co-occupying both types of adsorption sites.

Summary and Conclusions

The physisorption of a hydrogen molecule to a conjugated ring system has been studied by high-level ab initio methodology. This involves extension to large basis sets, which is achieved by the RI-MP2 scheme. It is also shown that RI-MP2

is able to reproduce the dispersion interaction energies calculated by the canonical theory within an insignificant margin of error. In addition, the basis set convergence is further improved by employing the full counterpoise correction scheme for removing the BSSE. RI-MP2 is also used to extend the calculations beyond the simplest model, which is the one-ring system.

Two different orientations of the adsorbed hydrogen molecule with respect to the benzene ring have been identified. The first involves the top site, where the hydrogen molecule is found to point with its axis toward the center of the plane. This is the stronger type of the considered sites, where the second type involves approach of the hydrogen molecule from the side of the plane. In this edge site the axis of the hydrogen molecule is found to point in a perpendicular orientation to the conjugation plane pointing toward a carbon–carbon bond of the conjugation skeletal. Our calculations support the interpretation of recent experimental data⁴⁵ on hydrogen uptake by MOFs suggesting the existence of the edge site and place it on a firmer ground.

The interaction of hydrogen molecule with the organic linker within MOFs has been further analyzed by employing RI-MP2 with larger models. These extended models involve dicarboxylated benzene ring and a two-ring molecule. The carboxylic groups are used in the synthesis of MOFs to bind the organic unit to the inorganic clusters. The calculated adsorption energies find that the top site involves a stronger interaction than the edge site as predicted from recent experimental observations. The adsorption energy of the top site is around 4 kJ/mol, where the edge site is more than 2 kJ/mol weaker. In addition, we find that the effect of the carboxylic groups on the adsorption energy is marginal (about 0.5 kJ/mol variances). These observations are changed when a modified ring structure is considered.

We have calculated the effect of modifying the carbon ring structure by introducing an electron donor–acceptor atom pair into the conjugation ring. This modified ring involves a pair of boron–nitrogen atoms replacing a carbon–carbon pair within the benzene ring. We have also calculated the effect of the carboxylic groups on the adsorption energies with this modified ring model. We observe that this chemical modification significantly influences the calculated adsorption energy of the edge site already for the one-ring model with over 2 kJ/mol enhancement of the interaction energy. Furthermore, with the carboxylic groups even stronger enhancements are predicted for both sites. With these models the adsorption energy of the edge site is over 5 kJ/mol and that for the top site is over 10 kJ/mol. These predictions of enhancing the weakest adsorption sites by a specific chemical manipulation may be crucial in finding new synthetic routes to further improve the uptake properties of related materials. This also confirms recent results on the interaction of hydrogen with MOF where it has been shown that the ability of the adsorbing molecule to polarize the guest molecule underlies the sorption interaction.²⁶

The effect of increasing the conjugation system size on hydrogen adsorption was also studied. A small enhancement of the top site by about 0.4 kJ/mol is calculated. This is in accordance with previous studies.^{28,29,31} Also predicted is a slightly enhancement of the edge site with increase of the conjugation system size. Even though some of our predictions

for the top site can be compared to previous studies, in this work we have also considered the edge site.

Future research should study the effect of co-loading several sites including populating the much stronger inorganic sites. This will involve employing even larger models that include the metal atoms of the inorganic cluster. This will allow not only focusing also on the stronger inorganic sites but also representing more faithfully their relation to the organic linker sites. Other organic linkers should be studied as well.

Acknowledgment. It is a pleasure to acknowledge valuable discussions with Dr. Omar M. Yaghi, Dr. Adam J. Matzger, and Dr. Wong F. Antek. We are also grateful to Robert DiStasio for providing assistance in using a prerelease version of the RI-MP2 code. B.D.D. acknowledges financial support from the University of Michigan. The Department of Energy, Office of Science, has generously allocated computational resources by the National Energy Research Scientific Computing Center for this project through a computational start-up fund.

References and Notes

- (1) Seayad, A. M.; Antonelli, D. M. *Adv. Mater.* **2004**, *16*, 765.
- (2) Schlappbach, L.; Anderson, I.; Burger, J. P. *Electronic and Magnetic Properties of Metals and Ceramics Part III*; VCH: Weinheim, Germany, 1994; Vol. 3B, p 271.
- (3) Perng, T. P.; Wu, J. K. *Mater. Lett.* **2003**, *57*, 3437.
- (4) Yamaguchi, M.; Akiba, E. *Electronic and Magnetic Properties of Metals and Ceramics Part II*; VCH: Weinheim, Germany, 1994; Vol. 3B, p 333.
- (5) Huot, J. *Nanoclusters and Nanocrystals*; American Scientific Publishers: Stevenson Ranch, CA, 2003; Chapter 2.
- (6) Dillon, C.; Jenes, K. M.; Bekkedehi, T. A.; Kiang, C. H.; Bethune, D. S.; Heben, M. J. *Nature* **1997**, *386*, 377.
- (7) Chen, P.; Wu, X.; Lin, J.; Tan, K. L. *Science* **1999**, *285*, 91.
- (8) Pinkerton, F. E.; Wicke, B. G.; Olk, C. H.; Tibbetts, G. G.; Meisner, G. P.; Meyer, M. S.; Herbst, J. F. *J. Phys. Chem. B* **2000**, *104*, 9460.
- (9) Liu, B.; Fan, Y. Y.; Liu, M.; Cong, H. T.; Cheng, H. M.; Dresselhaus, M. S. *Science* **1999**, *286*, 1127.
- (10) Pradhan, B. K. *J. Mater. Res.* **2002**, *17*, 2209.
- (11) Froudakis, G. E. *J. Phys.: Condens. Matter* **2002**, *14*, R453.
- (12) Abrahamas, B. F.; Hoskins, B. F.; Michail, D. M.; Robson, R. *Nature* **1994**, *369*, 727.
- (13) Mallouk, T. E. *Nature* **1997**, *387*, 350.
- (14) Liu, F. Q.; Tilley, T. D. *J. Chem. Soc., Chem. Commun.* **1998**, *98*, 103.
- (15) Li, H.; Eddaoudi, M.; O'Keefe, M.; Yaghi, O. M. *Nature* **1999**, *402*, 276.
- (16) Wu, C. D.; Hu, A.; Zhang, L.; Lin, W. B. *J. Am. Chem. Soc.* **2005**, *127*, 8940.
- (17) Rowsell, J. L. C.; Millward, A. R.; Park, K. S.; Yaghi, O. M. *J. Am. Chem. Soc.* **2004**, *126*, 5666.
- (18) Eddaoudi, M.; Kim, J.; Rosi, N.; Vodak, D.; Wachter, J.; O'Keefe, M.; Yaghi, O. M. *Science* **2002**, *295*, 469.
- (19) Rowsell, J. L. C.; Eckert, J.; Yaghi, O. M. *J. Am. Chem. Soc.* **2005**, *127*, 14904.
- (20) Chae, H. K.; Siberio-Perez, D. Y.; Kim, J.; Go, Y.; Eddaoudi, M.; Matzger, A. J.; O'Keefe, M.; Yaghi, O. M. *Nature* **2004**, *427*, 523.
- (21) Kepert, C. J. *Chem. Commun.* **2006**, 695.
- (22) Kitagawa, S.; Kitaura, R.; Noro, S. *Angew. Chem., Int. Ed.* **2004**, *43*, 2334.
- (23) Eddaoudi, M.; Moler, D. B.; Li, H.; Chen, B.; Reineke, T. M.; O'Keefe, M.; Yaghi, O. M. *Acc. Chem. Res.* **2001**, *34*, 319.
- (24) Rosseinski, M. J. *Microporous Mesoporous Mater.* **2004**, *73*, 15.
- (25) Mori, W.; Takamizawa, S.; Kato, C. N.; Ohmura, T.; Sato, T. *Microporous Mesoporous Mater.* **2004**, *73*, 31.
- (26) Centrone, A.; Siberio-Perez, D. Y.; Millward, A. R.; Yaghi, O. M.; Matzger, A. J.; Zerbi, G. *Chem. Phys. Lett.* **2005**, *411*, 516.
- (27) Eckert, J.; Nicol, J. M.; Howard, J.; Trouw, F. R. *J. Phys. Chem.* **1996**, *100*, 10646.
- (28) Tran, F.; Weber, J.; Wesolowski, T. A.; Cheikh, F.; Ellinger, Y.; Pauzat, F. *J. Phys. Chem. B* **2002**, *106*, 8689.
- (29) Heine, T.; Zhechkov, L.; Seifert, G. *Phys. Chem. Chem. Phys.* **2004**, *6*, 980.
- (30) Hamel, S.; Cote, M. J. *Chem. Phys.* **2004**, *121*, 12618.
- (31) Hubner, O.; Gloss, A.; Fichtner, M.; Kloppe, W. *J. Phys. Chem. A* **2004**, *108*, 3019.
- (32) Sagara, T.; Klassen, J.; Ganz, E. *J. Chem. Phys.* **2004**, *121*, 12543.
- (33) Sagara, T.; Klassen, J.; Ortony, J.; Ganz, E. *J. Chem. Phys.* **2005**, *123*, 014701-1.
- (34) (a) Becke, A. D. *J. Chem. Phys.* **1993**, *98*, 5648. (b) Vosko, S. H.; Wilk, L.; Nusair, M. *Can. J. Phys.* **1980**, *58*, 1200. (c) Lee, C.; Yang, W.; Parr, R. G. *Phys. Rev. B* **1988**, *37*, 785.
- (35) Dunning, T. H., Jr. *J. Chem. Phys.* **1989**, *90*, 1007.
- (36) Schaefer, A.; Huber, C.; Ahlrichs, R. *J. Chem. Phys.* **1994**, *100*, 5829.
- (37) (a) Feyereisen, M.; Fitzgerald, G.; Komornicki, A. *Chem. Phys. Lett.* **1993**, *208*, 359. (b) Weigend, F.; Haser, M. *Theor. Chem. Acc.* **1997**, *97*, 331. (c) Weigend, F.; Haser, M.; Patzelt, H.; Ahlrichs, R. *Chem. Phys. Lett.* **1998**, *294*, 143.
- (38) DiStasio, R. A., Jr.; Steele, R. P.; Rhee, Y. M.; Shao, Y.; Head-Gordon, M. Submitted for publication in *J. Comput. Chem.* **2006**.
- (39) Liu, B.; McLean, A. D. *J. Chem. Phys.* **1973**, *59*, 4557.
- (40) <http://www.chem-bio.uni-karlsruhe.de/TheoChem/turbomole/intro-.en.html>.
- (41) Schmidt, M. W.; Baldrige, K. K.; Boatz, J. A.; Elbert, S. T.; Gordon, M. S.; Jensen, J. H.; Koseki, S.; Matsunaga, N.; Nguyen, K. A.; Su, S.; Windus, T. L.; Dupuis, M.; Montgomery J. A. *J. Comput. Chem.* **1993**, *14*, 1347.
- (42) Kong, J.; White, C. A.; Krylov, A. I.; Sherrill, C. D.; Adamson, R. D.; Furlani, T. R.; Lee, M. S.; Lee, A. M.; Gwaltney, S. R.; Adams, T. R.; Ochsenfeld, C.; Gilbert, A. T. B.; Kedziora, G. S.; Rassolov, V. A.; Maurice, D. R.; Nair, N.; Shao, Y.; Besley, N. A.; Maslen, P. E.; Dombroski, J. P.; Daschel, H.; Zhang, W.; Korambath, P. P.; Baker, J.; Byrd, E. F. C.; Van Voorhis, T.; Oumi, M.; Hirata, S.; Hsu, C. P.; Ishikawa, N.; Florian, J.; Warshel, A.; Johnson, B. G.; Gill, P. M. W.; Head-Gordon, M.; Pople, J. A. *J. Comput. Chem.* **2000**, *21*, 1532.
- (43) Shao, Y.; Molnar, L. F.; Jung, Y.; Kussmann, J.; Ochsenfeld, C.; Brown, S. T.; Gilbert, A. T. B.; Slipchenko, L. V.; Levchenko, S. V.; O'Neill, D. P.; DiStasio, R. A., Jr.; Lochan, R. C.; Wang, T.; Beran, G. J. O.; Besley, N. A.; Herbert, J. M.; Lin, C. Y.; Van Voorhis, T.; Chien, S. H.; Sodt, A.; Steele, R. P.; Rassolov, V. A.; Maslen, P. E.; Korambath, P. P.; Adamson, R. D.; Austin, B.; Baker, J.; Byrd, E. F. C.; Daschel, H.; Doerksen, R. J.; Dreuw, A.; Dunietz, B. D.; Dutoi, A. D.; Furlani, T. R.; Gwaltney, S. R.; Heyden, A.; Hirata, S.; Hsu, C.; Kedziora, G.; Khalliulin, R. Z.; Klunzinger, P.; Lee, A. M.; Lee, M. S.; Liang, W.; Lotan, I.; Nair, N.; Peters, B.; Proynov, E. I.; Pieniazek, P. A.; Rhee, Y. M.; Ritchie, J.; Rosta, E.; Sherrill, C. D.; Simmonett, A. C.; Subotnik, J. E.; Woodcock, H. L., III; Zhang, W.; Bell, A. T.; Chakraborty, A. K.; Chipman, D. M.; Keil, F. J.; Warshel, A.; Hehre, W. J.; Schaefer, H. F., III; Kong, J.; Krylov, A. I.; Gill, P. M. W.; Head-Gordon, M. Submitted for publication in *Phys. Chem. Chem. Phys.*
- (44) *Jaguar 5.5*; Schrödinger, LLC.: Portland, OR, 2003.
- (45) Rowsell, J. L. C.; Spencer, E. C.; Eckert, J.; Howard, J. A. K.; Yaghi, O. M. *Science* **2005**, *309*, 1350.
- (46) Quinonero, D.; Garau, C.; Frontera, A.; Ballester, P.; Costa, A.; Deyá, P. M. *J. Phys. Chem. A* **2005**, *109*, 4632.
- (47) Private communication with Dr. Omar M. Yaghi.
- (48) (a) Ishii, T.; Sato, T.; Sekikawa, Y.; Iwata, M. *J. Cryst. Growth* **1981**, *52*, 285. (b) Ma, R.; Bando, Y.; Sato, T. *Adv. Mater.* **2002**, *14*, 366. (c) Wang, P.; Orimo, S.; Matsushima, T.; Fujii, H.; Majer, G. *Appl. Phys. Lett.* **2002**, *80*, 318. (d) Tang, C.; Bando, Y.; Ding, X.; Qi, S.; Golberg, D. *J. Am. Chem. Soc.* **2002**, *124*, 14550.
- (49) Kristyan, S.; Pulay, P. *Chem. Phys. Lett.* **1994**, *229*, 175.